Published in final edited form as:
J Org Chem. 2009 October 16; 74(20): 7834–7843. doi:10.1021/jo901594e.

Conformational preferences of 1-amino-2-phenylcyclohexanecarboxylic acid, a phenylalanine cyclohexane analogue

Carlos Alemán[1,2,*], **Ana I. Jiménez**[3], **Carlos Cativiela**[3], **Ruth Nussinov**[4,5], and **Jordi Casanovas**[6,*]

[1] Departament d'Enginyeria Química, E. T. S. d'Enginyeria Industrial de Barcelona, Universitat Politècnica de Catalunya, Diagonal 647, Barcelona E-08028, Spain

[2] Center for Research in Nano-Engineering, Universitat Politècnica de Catalunya, Campus Sud, Edifici C', C/Pasqual i Vila s/n, Barcelona E-08028, Spain

[3] Departamento de Química Orgánica, Instituto de Ciencia de Materiales de Aragón, Universidad de Zaragoza – CSIC, 50009 Zaragoza, Spain

[4] Basic Research Program, SAIC-Frederick, Inc. Center for Cancer Research Nanobiology Program, NCI, Frederick, MD 21702, USA

[5] Department of Human Genetics Sackler, Medical School, Tel Aviv University, Tel Aviv 69978, Israel

[6] Departament de Química, Escola Politècnica Superior, Universitat de Lleida, c/Jaume II n^{o} 69, Lleida E-25001, Spain

Abstract

The intrinsic conformational preferences of the restricted phenylalanine analogue generated by including the α and β carbon atoms into a cyclohexane ring (1-amino-2-phenylcyclohexanecarboxylic acid, c_6Phe) have been determined using quantum mechanical calculations. Specifically, the conformational profile of the *N*-acetyl-*N*'-methylamide derivative of the c_6Phe stereoisomers exhibiting either a *cis* or a *trans* relative orientation between the amino and phenyl substituents has been analyzed in different environments (gas phase, chloroform and aqueous solutions). Calculations were performed using B3LYP, MP2 and HF methods combined with the 6-31+G(d,p) and 6-311++G(d,p) basis sets, and a self-consistent reaction-field (SCRF) method was applied to analyze the influence of the solvent. The amino acids investigated can be viewed as constrained phenylalanine analogues with a rigidly oriented aromatic side chain that may interact with the peptide backbone not only sterically but also electronically through the aromatic π orbitals. Their conformational propensities have been found to be strongly influenced by the specific orientation of the aromatic substituent in each stereoisomer and the conformation adopted by the cyclohexane ring, as well as by the environment.

*carlos.aleman@upc.edu and jcasanovas@quimica.udl.cat.

Supporting Information Available

Coordinates and energy of the minimum energy conformations characterized for Ac-*c*-L-c_6Phe-NHMe and Ac-*t*-L-c_6Phe-NHMe. This material is available free of charge via the Internet at http://pubs.acs.org.

Introduction

The incorporation of restricted amino acids into peptide chains is a powerful tool for the construction of peptide analogues with well-defined three-dimensional arrangements. α,α-Dialkylated residues are particularly useful because tetrasubstitution at the α carbon severely restricts the conformational space available to the peptide backbone and this leads to the stabilization of certain elements of secondary structure.[1] Thus, the simplest α,α-dialkylated amino acid, (α-methyl)alanine (also known as α-aminoisobutyric acid, Aib) is found almost exclusively in the 3_{10}-/α-helical region of the Ramachandran map.[1] In comparison, higher homologues of Aib with linear side chains prefer the fully-extended conformation, whereas their cyclic counterparts, 1-aminocycloalkanecarboxylic acids (Ac_nc), strictly parallel the behavior of Aib, with some distortion in the case of the highly strained cyclopropane derivative (n = 3).[1]

The repertoire of non-natural amino acids useful in peptide design may be expanded by attaching a substituent to the cycloalkane moiety of Ac_nc. This combines the presence of side-chain functionality, which may be essential for peptide-receptor recognition when dealing with a bioactive peptide, with the well-defined conformational properties of the Ac_nc residues. The new side-chain functionality incorporated may be selectively oriented by selecting a certain cycloalkane size and stereochemistry. Given that side chains are directly involved in molecular recognition processes, their three-dimensional arrangement is crucial for adequate peptide-receptor interaction. Moreover, side chains may play a role in directing the conformational preferences of the peptide backbone.[2]

In recent years, we have been working on the synthesis[3] and structural study[4] –both theoretically and experimentally– of the amino acids obtained by incorporating a phenyl substituent at one of the β carbons of Ac_nc for n = 3–6. The compounds thus generated are phenylalanine (Phe) analogues and we designate them as c_nPhe, where n refers to the ring size, as in Ac_nc. The cyclic nature of the c_nPhe residues precludes rotation about the C^{α}—C^{β} bond and the orientation of the aromatic side chain is therefore dictated by the size (n value) and stereochemistry of the cycloalkane ring. It should be noted that the phenyl substituent incorporated at the β position may exhibit either a *cis* or a *trans* relative orientation with respect to the amino function, respectively giving rise to *cis*- or *trans*-c_nPhe derivatives. The c_nPhe residues with diverse ring size and stereochemistry constitute a set of phenylalanine analogues with distinct well-defined side-chain arrangements. They are excellent tools to investigate the ability of the side chain to influence the peptide backbone conformation[4] since the tightly held aromatic substituent may interact with the backbone not only sterically but also electronically through the aromatic π orbitals. Indeed, the different spatial orientation attained by the aromatic substituent in the c_nPhe residues has proven useful in several applications related to the stabilization of particular peptide backbone conformations.[4,5]

In particular, we have shown that the cyclohexane members (c_6Phe) are able to stabilize different types of β-turns depending on the phenyl side-chain orientation,[4b,e] at variance with the behavior exhibited by the natural amino acid.[4e,f] These experimental results prove that the phenylalanine cyclohexane analogues (c_6Phe) are able to modulate the peptide backbone conformation, and show therefore great promise as phenylalanine substitutes in the design of peptides with controlled fold in the backbone. In early studies, molecular mechanics (MM) simulations were used to explore the conformational propensities of c_6Phe.[4d] The minimum energy conformations located were subsequently used as starting points for energy minimizations at the HF/6-31G(d) quantum mechanical level. However, such a study cannot be considered as a complete description of the conformational propensities of c_6Phe due to the intrinsic limitations associated with MM methods. As a matter of fact, only 7 and 8 minima were characterized for the *N*-acetyl-*N'*-methylamide derivatives of *cis*-c_6Phe and *trans*-c_6Phe,

respectively, in that MM study,[4d] whereas the number of minima expected for these compounds is significantly higher. The reason for this is that quantum mechanical calculations provided as many as 11 different minima for the analogous unsubstituted Ac_6c derivative.[6] Incorporation of a phenyl substituent into Ac_6c to generate *cis*- or *trans*-c_6Phe is expected to increase the number of minima because the symmetry of the molecule is broken [conformations characterized by (φ,ψ) and (–φ,–ψ) dihedral angles are equivalent for an achiral amino acid such as Ac_6c but not for the non-symmetrical c_6Phe residues], and therefore each minimum energy conformation characterized for Ac_6c should translate, in principle, into two different c_6Phe minima. Obviously, some of the expected minima may be annihilated, in the same way as new minima without precedent in Ac_6c may appear in c_6Phe induced by the presence of the aromatic substituent. In this context, a comparison with the cyclopentane series is instructive: quantum mechanical calculations provided 5 minimum energy conformations for Ac_5c,[7] while 8 and 10 minima, respectively, were located for *cis*-c_5Phe and *trans*-c_5Phe.[4a]

In this work, we present a complete conformational study of the *N*-acetyl-*N'*-methylamide derivatives of the cyclohexane analogues of L-phenylalanine exhibiting a *cis* or a *trans* relative orientation between the phenyl substituent and the amino function, hereafter denoted as Ac-*c*-$_L$-c_6Phe-NHMe and Ac-*t*-$_L$-c_6Phe-NHMe, respectively (Figure 1a). Density functional theory (DFT) calculations at the B3LYP/6-31+G(d,p) level have been used to locate and characterize the minimum energy conformations for these compounds. In order to obtain reliable estimates, the relative energies of all these structures have been re-evaluated using different theoretical levels. Moreover, the influence of the solvent on the conformational preferences of the compounds under study has been analyzed using a self-consistent reaction-field (SCRF) method. The intrinsic conformational preferences calculated in the present work for the c_6Phe derivatives have been compared with those described recently for the unsubstituted Ac_6c residue.[6]

Methods

All the calculations were performed using the Gaussian 03 computer program.[8] In order to characterize the minimum energy conformations of Ac-*c*-$_L$-c_6Phe-NHMe and Ac-*t*-$_L$-c_6Phe-NHMe, a systematic exploration of the conformational space was performed. Given that each flexible backbone dihedral angle (φ,ψ) is expected to exhibit three minima, 9 minima can be anticipated for the potential energy surface $E=E(\varphi,\psi)$. Regarding the cyclohexane ring, the two possible chair conformations (Figure 1b) were initially considered for each compound. Additionally, two half-chairs (Figure 1b) were included as starting geometries. Although the latter arrangement is very high in energy and is not expected to be found in any energy minima, it is a good starting point to explore cyclohexane conformations different from chair, such as boat or twist. Accordingly, for each c_6Phe derivative under study, 9 (φ,ψ minima) × 4 (2 chair + 2 half-chair cyclohexane conformations) = 36 structures were used as starting points for subsequent full geometry optimizations.

All geometry optimizations were performed using the B3LYP functional[9,10] combined with the 6-31+G(d,p) basis set,[11] *i.e.* B3LYP/6-31+G(d,p). Frequency analyses were carried out to verify the nature of the minimum state of all the stationary points obtained and to calculate the zero-point vibrational energies (ZPVE) and both thermal and entropic corrections. These statistical terms were then used to compute the conformational Gibbs free energies in the gas phase at 298K (ΔG_{gp}). To analyze the influence of the size of the basis set and the theoretical method used on the conformational energies, single point calculations at the HF/6-31+G(d,p), MP2/6-31+G(d,p),[12] and B3LYP/6-311++G(d,p)[13] levels were further performed on all the minima.

To obtain an estimation of the solvation effects on the relative stability of the most relevant minima, single-point calculations were conducted on the optimized structures using a SCRF model. Specifically, the Polarizable Continuum Model (PCM) developed by Tomasi and co-workers[14] was used to describe chloroform and water as solvents. The PCM method represents the polarization of the liquid by a charge density appearing on the surface of the cavity created in the solvent. This cavity is built using a molecular shape algorithm. PCM calculations were performed in the framework of the B3LYP/6-31+G(d,p) level using the standard protocol and considering the dielectric constants of chloroform (ε = 4.9) and water (ε = 78.4) to obtain the free energies of solvation (ΔG_{solv}) of the minimum energy conformations. Within this context, it should be emphasized that previous studies indicated that solute geometry relaxations in solution and single-point calculations on the optimized geometries in the gas phase give almost identical ΔG_{solv} values.[15] The conformational free energies in solution (ΔG_{Chl} and ΔG_{water}) at the B3LYP/6-31+G(d,p) level were then estimated using the classical thermodynamics scheme, *i.e.* by adding the ΔG_{solv} and ΔG_{gp} values.

Results and Discussion

Complete geometry optimizations and frequency calculations led to the characterization of 17 and 21 minimum energy conformations in the gas phase for Ac-*c*-L-c_6Phe-NHMe and Ac-*t*-L-c_6Phe-NHMe, respectively. They are listed in Tables 1 and 2, where the conformation adopted by the peptide backbone and the cyclohexane ring, as well as the relative energy (ΔE_{gp}) and free energy (ΔG_{gp}) calculated at the B3LYP/6-31+G(d,p) level are indicated for each minimum. Perczel's nomenclature[16] has been used to identify the different peptide backbone conformations.

Ac-c_L-c_6Phe-NHMe

The 17 minimum energy conformations characterized for this compound in the gas phase are distributed within a relative energy interval of 13.9 kcal/mol (Table 1). Eight of them present ΔE_{gp} values lower than 6 kcal/mol, and are depicted in Figure 2. The contribution of the remaining minima in Table 1 to the conformational equilibrium of Ac-*c*-L-c_6Phe-NHMe is expected to be negligible not only in the gas phase but also in solution, given that solute-solvent interactions typically mean a stabilization of several kcal/mol.

The lowest energy minimum of Ac-*c*-L-c_6Phe-NHMe (**1**) adopts a γ_L backbone arrangement (inverse γ-turn or equatorial C_7 conformation), in which the terminal acetyl CO and methylamide NH sites form an intramolecular hydrogen bond [d(H···O)= 1.929 Å, <N–H···O= 154.2°] defining a seven-membered cycle (Figure 2a). In this conformation, the phenyl substituent and the amino group of *cis*-c_6Phe lie in close proximity, thus allowing the formation of a weak attractive interaction of the N–H···π type. The geometry of this interaction is defined by the distance between the amide hydrogen and the center of the aromatic system ($d_{H\cdots Ph}$= 3.248 Å) and the angle formed by the N–H bond and the phenyl ring plane (θ= 18.1°). The ability of the π electron density of aromatic systems to interact with proton donors has long been recognized,[17] and more recently has been identified as a stabilizing factor of peptide and protein structures.[18] Importantly, interactions of this type have been observed experimentally in small peptides containing c_3Phe[4f] and c_6Phe,[4e] and characterized theoretically for the former residue.[4c]

The same γ_L backbone conformation is found in minima **2** and **3**, which are stabilized by similar hydrogen bonding and NH-aromatic interactions (Figures 2b and 2c). Indeed, the three γ_L structures in Table 1 differ mainly in the shape of the cyclohexane ring. The global minimum presents a chair of type I (Figure 1b), which is expected to be that preferred by Ac-*c*-L-c_6Phe-NHMe according to the axial/equatorial arrangement of the substituents and the tendency of bulky groups to avoid axial positions because they are known to produce a higher steric

hindrance with the rest of the cyclohexane system. In chair I, the bulky phenyl ring is equatorially located and only one of the three cyclohexane substituents (–NHCOMe) occupies an axial position. In minimum **2**, the six-membered ring assumes the alternate chair arrangement (II, Figure 1b), that bears the phenyl and –CONHMe groups in axial whereas the amino moiety occupies an equatorial position. The less favorable orientation of the cyclohexane substituents in this case is associated to an energy penalty of 2.6 kcal/mol in terms of ΔE_{gp}. It is highly remarkable that the six-membered ring in minimum **3** adopts a twist conformation, that is, a slightly distorted boat. The high stability of this structure, which is only 0.5 kcal/mol above minimum **2**, may be related to the presence of two substituents –among which is the sterically more demanding one (the phenyl group)– in pseudoequatorial positions, and the non-existence of steric conflicts between the peptide backbone and either the cyclohexane moiety or the phenyl substituent.

The next two minima, **4** (Figure 2d) and **5** (Figure 2e), also exhibit a hydrogen bond linking the terminal acetyl CO and methylamide NH groups and closing the seven-membered cycle typical of a γ-turn. However, in this case, the sign of the (φ,ψ) dihedral angles corresponds to a γ_D conformation (axial C_7 or classical γ-turn). Inversion of the γ-turn type results in the disruption of the interaction between the aromatic π orbitals and the *cis*-c_6Phe NH site. Moreover, only chair arrangements of the cyclohexane ring are found to be compatible with this backbone conformation. Surprisingly enough, the most stable γ_D minimum (**4**) presents a type II chair, with the bulky phenyl group located axially. The *a priori* unexpected higher stability observed for this conformer is due to the fact that chair I in **5** brings in close proximity the acetyl oxygen atom of the –NHCOMe peptide fragment and the aromatic ring, thus introducing a very strong steric and electronic repulsion. To minimize this repulsive interaction, the peptide backbone geometry in minimum **5**, (φ,ψ) = (47,–14), is highly distorted with respect to that corresponding to a standard γ_D conformation, (φ,ψ) ≈ (70,–60).

The unfavorable interactions between the –NHCOMe oxygen and the phenyl substituent for a chair I-shaped cyclohexane are not present when the peptide backbone assumes semi-extended or fully-extended structures characterized by large ψ values. Thus, minima **6** and **7** combine, respectively, an ε_L (also called polyproline II) or a β_L (C_5) conformation with a chair I disposition for the cyclohexane ring. In contrast, none of these backbone arrangements seem to be compatible with chair II (Table 1). Minimum **6** (Figure 2f) lacks stabilizing interactions either of the hydrogen bond or N–H···π type, whereas a weak intramolecular hydrogen bond [d(H···O)= 1.907 Å, <N–H···O= 118.2°] connecting the amide functions is present in **7** (Figure 2g). It is interesting to note that **6** presents a ΔG_{gp} value considerably low (3.8 kcal/mol), and is the fourth most stable minima –instead of the sixth– in terms of relative free energy.

The last conformer in Figure 2 (**8**, Figure 2h) exhibits a ΔE_{gp} value of 5.7 kcal/mol and falls into the left-handed α-helix region (α_D) of the Ramachandran map. This backbone conformation combined with a cyclohexane chair II arrangement allows the formation of a stabilizing interaction between the π cloud of the axially-oriented phenyl ring and the NH group of *cis*-c_6Phe. Although not included in Figure 2, a minimum with an α_L backbone geometry and very close in energy (**9**, Table 1) was also characterized. Notably enough, none of the α-helical minima located present a cyclohexane accommodating the alternate chair conformation.

Ac-t-L-c_6Phe-NHMe

Table 2 describes the most relevant geometrical parameters corresponding to the 21 minimum energy conformations characterized for the *trans*-c_6Phe derivative in the gas phase, which show ΔE_{gp} and ΔG_{gp} values of up to 14.6 and 14.4 kcal/mol, respectively. The 8 most stable minima are displayed in Figure 3.

As observed before for the *cis*-c_6Phe derivative, the global minimum of Ac-*t*-$_L$-c_6Phe-NHMe (**1**, Figure 3a) combines a γ_L backbone conformation and a cyclohexane ring assuming the most favorable chair arrangement, namely that with the bulky aromatic substituent equatorially located (chair IV, Figure 1b). This structure is stabilized by the intramolecular hydrogen bond typical of the γ-turn conformation and by an NH-aromatic interaction, with geometrical parameters similar to those described for the global minimum of *cis*-c_6Phe.

Other energy minima exhibiting a γ_L backbone and differing from the global minimum in the cyclohexane shape were also located for Ac-*t*-$_L$-c_6Phe-NHMe (Table 2). However, in this case, reversal of the chair type from IV to III results in a destabilization of 6.9 kcal/mol (minimum **9**). Also a six-membered ring with a twist arrangement was found to be compatible with the γ_L structure for this compound, but at a high energy cost (minima **12** and **16**). This is in sharp contrast to that described before for Ac-*c*-$_L$-c_6Phe-NHMe. Thus, although *cis*- and *trans*-c_6Phe present global minima with high structural similarity, their response to changes in the cyclohexane conformation for this backbone disposition is notably different. The reason for this distinct behavior lies in the relative orientation of the phenyl ring, which for the *trans* derivative is next to the carboxyl terminus. Thus, the chair III arrangement combined with a γ_L backbone conformation (minimum **9**) results in a high proximity between the carbonyl oxygen of *trans*-c_6Phe and the aromatic substituent.

A parallel situation, although less marked, is found when comparing the minima exhibiting a γ_D structure for Ac-*c*-$_L$-c_6Phe-NHMe and Ac-*t*-$_L$-c_6Phe-NHMe. Thus, for the latter compound, changing the most favorable cyclohexane arrangement for this backbone (chair III, minimum **3**) to other shapes results in an energy increase of at least 2.4 kcal/mol. In comparison, for the *cis* derivative, the two alternate chairs are separated by an energy gap of 1.2 kcal/mol for the same γ_D conformation. Interestingly, for both compounds, this backbone type is more stable when combined with the chair bearing the aromatic substituent in axial (II for *cis*-c_6Phe and III for *trans*-c_6Phe).

Another remarkable feature in Table 2 is that three different conformational regions are visited by the minima with ΔE_{gp} below 5 kcal/mol, namely γ, β and δ. In comparison, only the former appears in Table 1 for the same energy limit. This indicates that the presence of the phenyl substituent produces a less severe restriction of the peptide backbone flexibility for the *trans* compound, at least, in the gas phase. A similar trend was observed for the c_3Phe[4c] and c_5Phe[4a] residues investigated before, indicating that the introduction of a phenyl group in Ac$_n$c to give the corresponding c$_n$Phe analogue produces more intense conformational constraints when the aromatic substituent is located in the neighborhood of the amino moiety (*cis*-c$_n$Phe).

The location of δ minima for the *trans*-c_6Phe derivative at about 4 kcal/mol (minima **4** and **5**) is noteworthy, since this type of peptide backbone geometry was not detected among the energy minima of the c$_n$Phe residues studied before.[4a,c] Although minima with a δ structure are also present in Table 1 for *cis*-c_6Phe, their relative energy is much higher (7.9 kcal/mol and above). The same holds true for the fully-extended conformation (β). Indeed, minimum **2** in Table 2 exhibits the intramolecularly hydrogen-bonded five-membered ring [d(H···O)= 1.961 Å, <N–H···O= 114.4°] typical of a β backbone conformation, and is destabilized with respect to the global minimum by only 2.7 kcal/mol. In comparison, the most stable structure with a β backbone found for Ac-*c*-$_L$-c_6Phe-NHMe is 5.6 kcal/mol less stable than the lowest energy minimum. This distinct behavior must be ascribed to the different steric hindrance produced between the cyclohexane ring (the axial hydrogen atoms attached to the γ and γ' carbons, mainly) and the –NHCOMe or –CONHMe peptide fragments when the latter are axially located (as occurs in the chairs of the most stable β conformers of *cis*- c_6Phe and *trans*-c_6Phe, respectively) and adopt a fully-extended conformation, that is, φ and ψ angles close to 180°.

Influence of the thermodynamic corrections, the quantum mechanical method and the basis set on the relative stabilities

Figure 4 represents ΔE_{gp} *vs*. ΔG_{gp} for the minimum energy conformations of Ac-*c*-L-c_6Phe-NHMe and Ac-*t*-L-c_6Phe-NHMe at the B3LYP/6-31+G(d,p) level of theory (Tables 1 and 2). As can be seen, there is a strong correlation between the two parameters, the incorporation of ZPVE, thermal, and entropic corrections leading to a systematic reduction of the ΔE_{gp} values. Thus, ΔG_{gp} is on average 7% lower than ΔE_{gp}, with an average reduction of 9% and 6%, respectively, for the *cis* and *trans* derivatives.

Tables 3 and 4 compare the ΔE_{gp} values calculated for the compounds under study at different theoretical levels: B3LYP/6-31+G(d,p), MP2/6-31+G(d,p), HF/6-31+G(d,p) and B3LYP/6-311++G(d,p), with molecular geometries optimized at the B3LYP/6-31+G(d,p) level in all cases. Comparison of the results obtained using the B3LYP and MP2 methods combined with the 6-31+G(d,p) basis set (Figure 5a) reveals an excellent agreement. Thus, the ΔE_{gp} values provided by the former method are overestimated by about 11–13% only. The difference between these two methods should be mainly attributed to the N–H···π interaction, which is better described at the MP2 level, because the strength of interactions involving the π cloud of aromatic systems is typically underestimated by the B3LYP functional.[15] A very significant concordance is also displayed by the ΔE_{gp} values calculated using the B3LYP and HF methods combined with the 6-31+G(d,p) basis set (Figure 5b). On the other hand, the negligible influence of the size of the basis set is reflected in Figure 5c, which compares the ΔE_{gp} values obtained using the B3LYP functional combined with the 6-31+G(d,p) and 6-311++G(d,p) basis sets. The overall of these results indicates that the B3LYP/6-31+G(d,p) theoretical level is suitable for the evaluation of energies in the gas phase.

Influence of the solvent

The influence of chloroform and water on the conformational preferences of the c_6Phe derivatives was evaluated using the PCM method. The conformational free energy in a given solvent was approximated by adding ΔG_{solv} to the best estimation of ΔG_{gp}, which is abbreviated as $\Delta G_{gp,*}$ and was determined by combining the ΔE_{gp} value calculated at the MP2/6-31+G(d,p) level with the thermodynamic corrections obtained at the B3LYP/6-31+G(d,p) level. The values of $\Delta G_{gp,*}$ and the conformational free energies in chloroform and aqueous solutions (ΔG_{Chl} and ΔG_{water}, respectively) for all the minimum energy conformations of Ac-*c*-L-c_6Phe-NHMe and Ac-*t*-L-c_6Phe-NHMe are given in Tables 5 and 6, respectively. In general, the solvent plays a stabilizing role, which is reflected by a reduction of the relative free energies interval. Specifically, for Ac-*c*-L-c_6Phe-NHMe, the $\Delta G_{gp,*}$ interval is wider than the ΔG_{Chl} and ΔG_{water} ones by 2.5 and 2.1 kcal/mol, respectively. For Ac-*t*-L-c_6Phe-NHMe, this feature is detected in chloroform solution only (1.6 kcal/mol). It is also interesting to note that the $\Delta G_{gp,*}$ value for some conformers is significantly lower than that of ΔG_{gp} provided in Tables 1 and 2.

Furthermore, solvation induces important changes in the stability order of the different conformers. Thus, **6** and **8** become the most favored structures for the *cis*-c_6Phe derivative in chloroform (Table 5). Although the relative stability of **1** decreases significantly in this organic solvent (ΔG_{Chl}= 0.6 kcal/mol), it is still significantly populated at room temperature. Indeed, the populations of **6**, **8** and **1** in chloroform according to a Boltzmann distribution are 44.3%, 37.3% and 15.5%, respectively. The stability of **8** increases with the polarity of the environment, and it becomes the lowest energy minimum in aqueous solution, with an estimated population of 77.3%. Conformer **6** is unfavored by 0.8 kcal/mol in water and accounts for 20.0% of the population, while the 15 remaining minima contribute by 2.7% only. Thus, the conformation preferred by Ac-*c*-L-c_6Phe-NHMe moves from the γ-turn in the gas phase to structures lacking an intramolecular hydrogen bond, namely polyproline II and α-helix, in

condensed phases. It should be noted that conformers with the six-membered ring arranged in twist are destabilized by more than 4.5 kcal/mol in solution, with **13** being the only exception. This conformer exhibits ΔG_{Chl}= 2.6 kcal/mol and ΔG_{water}= 2.0 kcal/mol, which correspond to an estimated population of 0.5% and 2.6% in chloroform and water, respectively.

The data in Table 6 reveal that the conformational flexibility of Ac-*t*-L-c_6Phe-NHMe is greatly increased by the presence of chloroform. Thus, seven structures are predicted to present significant populations in this organic solvent, namely **8** (36.6%), **5** (26.1%), **2** (9.3%), **3** (8.2%), **7** (8.0%), **1** (6.9%), and **11** (3.0%). In comparison, only **8** (66.7%) and **11** (29.7%) are expected to be significantly populated (≥ 3.0%) in aqueous solution. Accordingly, almost all types of peptide backbone arrangements are accessible to Ac-*t*-L-c_6Phe-NHMe in chloroform, whereas only the α-helical structure (either of the α_L or α_D type) is expected to be present in aqueous solution. Regarding the cyclohexane ring, although the structures exhibiting a twist arrangement are, in general, stabilized by the solvent, they present ΔG_{Chl} and ΔG_{water} values above 5.4 kcal/mol, and their populations remain, therefore, negligible at room temperature.

It should be mentioned that the X-ray crystalline structures of small peptides incorporating the c_6Phe residues[4b,e] actually show conformations corresponding to the α-helical region (occasionally, with some distortion induced by a contiguous proline), which is in agreement with the conformational preferences predicted for the two compounds under study in aqueous solution. In the solid state, the amide moieties of the peptide backbone may interact with the complementary CO and NH sites of neighboring molecules and, as a consequence, intra- and intermolecular hydrogen bonding compete, as happens in the presence of a solvent able to form hydrogen bonds with the peptide.

It is also noteworthy that the great influence exerted by the environment on the conformational preferences of the c_6Phe derivatives under study differs significantly from the behavior observed before for other c_nPhe residues. Thus, solvation was found to alter the conformational profiles of c_3Phe[4c] and c_5Phe[4a] from a quantitative point of view but not qualitatively and, indeed, the most populated conformations for these residues in the gas-phase were also found to be preferred in aqueous solution.

Comparison with the unsubstituted Ac_6c residue

Figure 6 represents a Ramachandran map comparing the distribution of the minimum energy conformations found for Ac-*c*-L-c_6Phe-NHMe and Ac-*t*-L-c_6Phe-NHMe in the present work (Tables 1 and 2) and those characterized before for the analogous Ac_6c derivative, Ac-Ac_6c-NHMe, at the same level of theory.[6] A color code has been used to identify the stability range of the different minima, which have been classified into three categories: $\Delta G_{gp} < 5$ kcal/mol (red), 5 kcal/mol ≤ $\Delta G_{gp} < 10$ kcal/mol (blue) and $\Delta G_{gp} \geq 10$ kcal/mol (yellow).

The incorporation of the phenyl side group, either in *cis* or in *trans* with respect to the amino terminus, produces a drastic reduction in the conformational diversity accessible to the peptide main chain. Thus, for Ac-Ac_6c-NHMe, four different types of backbone arrangements (namely, γ, α, ε, and β, with the L and D forms being energetically indistinguishable) were found within a ΔG_{gp} interval of 2.1 kcal/mol above the global minimum.[6] In contrast, only the γ_L conformation appears below this energy level for the two c_6Phe derivatives (Tables 1 and 2). The effect is particularly pronounced in the case of the *cis* compound, for which the most stable conformer with a peptide backbone other than γ_L exhibits a ΔG_{gp} value of 3.8 kcal/mol.

The destabilization induced by the aromatic substituent is clearly seen when comparing the minimum energy structures located in the α-helix region. The most stable minimum of this type found for Ac-Ac_6c-NHMe[6] presents the cyclohexane ring in a chair conformation with the –NHCOMe substituent axially oriented and shows a ΔG_{gp} value of 1.6 kcal/mol. In

comparison, the most stable α-helical minima characterized for Ac-*c*-L-c_6Phe-NHMe (Table 1) and Ac-*t*-L-c_6Phe-NHMe (Table 2) display ΔG_{gp} values of 5.4 and 6.3 kcal/mol, respectively. Moreover, in the Ac_6c derivative, reversal of the cyclohexane chair leads to another α-helical minimum 1.9 kcal/mol higher in energy. In contrast, only one chair is compatible with each type of α-helical backbone arrangement for the c_6Phe-containing compounds.

Minima exhibiting a twist-shaped cyclohexane ring were characterized for some backbone types in Ac_6c, with the α-helix not among these.[6] In contrast, such twist conformations are found to be compatible with the α-helix for both *cis*- and *trans*-c_6Phe. Moreover, in the case of the *cis* compound, a twist minimum was characterized at a ΔG_{gp} value as low as 3.4 kcal/mol (Table 1), whereas the most stable twist arrangement for Ac_6c exhibits a ΔG_{gp} value close to 6 kcal/mol.[6]

The incorporation of the phenyl substituent produces other effects, such as the modification of the geometry of minima with an ε backbone conformation. Minima of this type were characterized for Ac-Ac_6c-NHMe[6] with a chair-shaped cyclohexane at (φ,ψ) angles near (–60,120), or the equivalent (60,–120). When a phenyl group is incorporated in *cis* with the amino moiety, repulsive interactions arise between the aromatic group and the carbonyl oxygen of either the –NHCOMe or the –CONHMe substituent, depending on the ε_D or ε_L backbone type, respectively. To alleviate these, the φ or ψ angle, respectively, deviates by about 30° from the value observed in Ac_6c. Accordingly, the ε_D and ε_L minima in Ac-*c*-L-c_6Phe-NHMe with a cyclohexane ring arranged as a chair appear at (33,–124) and (–64,162), respectively (Table 1).

Conclusions

Quantum mechanical calculations have been used to characterize the intrinsic conformational preferences of Ac-*c*-L-c_6Phe-NHMe and Ac-*t*-L-c_6Phe-NHMe, incorporating the cyclohexane analogues of phenylalanine that bear the aromatic substituent in a *cis* or a *trans* orientation, respectively, relative to the amino group. A total of 17 and 21 energy minima have been found and characterized using B3LYP/6-31+G(d,p) calculations for Ac-*c*-L-c_6Phe-NHMe and Ac-*t*-L-c_6Phe-NHMe, respectively. Single point calculations at the MP2/6-31+G(d,p), HF/6-31+G(d,p), and B3LYP/6-311++G(d,p) levels were also performed. In the gas phase, the only significantly populated structures at room temperature for both compounds are those exhibiting a γ_L backbone conformation. Comparison with the results previously reported for the unsubstituted cyclohexane residue (Ac_6c) provides evidence for the ability of the aromatic group to interact with the peptide backbone not only sterically but also electronically through the aromatic π orbitals. Moreover, the additional phenyl group exerts a strong influence on the conformational equilibrium of the cyclohexane ring, which, in turn, affects the peptide backbone arrangement. As a consequence, the incorporation of the aromatic group in Ac_6c induces a severe restriction of the peptide backbone flexibility, which, in the gas phase, is less intense for the *trans* than for the *cis* c_6Phe analogue.

Solvation effects have been considered through a SCRF method and have been shown to alter significantly the conformational preferences of the c_6Phe derivatives under study. Thus, in aqueous solution, structures lacking any intramolecular hydrogen bond, such as polyproline II and α-helix, are preferred. It should be noted that the conformational preferences predicted in this environment are in agreement with the experimental data available from X-ray diffraction structures of small peptides containing the c_6Phe residues investigated.

Supplementary Material

Refer to Web version on PubMed Central for supplementary material.

Acknowledgments

Gratitude is expressed to the Centre de Supercomputació de Catalunya (CESCA) for computational facilities. Financial support from the Ministerio de Educación y Ciencia - FEDER (project CTQ2007-62245), Gobierno de Aragón (research group E40) and Generalitat de Catalunya (research group 2009 SGR 925) is gratefully acknowledged. Support for the research of C.A. was received through the prize "ICREA Academia" for excellence in research funded by the Generalitat de Catalunya. This project has been funded in whole or in part with Federal funds from the National Cancer Institute, National Institutes of Health, under contract number N01-CO-12400. The content of this publication does not necessarily reflect the view of the policies of the Department of Health and Human Services, nor does mention of trade names, commercial products, or organization imply endorsement by the U.S. Government. This research was supported [in part] by the Intramural Research Program of the NIH, National Cancer Institute, Center for Cancer Research.

References

1. a Toniolo C, Formaggio F, Kaptein B, Broxterman QB. Synlett 2006:1295. b Venkatraman J, Shankaramma SC, Balaram P. Chem. Rev 2001;101:3131. [PubMed: 11710065] c Toniolo C, Crisma M, Formaggio F, Peggion C. Biopolymers (Pept. Sci.) 2001;60:396. d Karle IL. Biopolymers (Pept. Sci.) 2001;60:351. e Kaul R, Balaram P. Bioorg. Med. Chem 1999;7:105. [PubMed: 10199661] f Karle IL. Acc. Chem. Res 1999;32:693. g Benedetti E. Biopolymers (Pept. Sci.) 1996;40:3. h Toniolo C, Benedetti E. Macromolecules 1991;24:4004.
2. Chakrabarti P, Pal D. Prog. Biophys. Mol. Biol 2001;76:1. [PubMed: 11389934]
3. Lasa M, Cativiela C. Synlett 2006:2517.references therein
4. a Casanovas J, Jiménez AI, Cativiela C, Nussinov R, Alemán C. J. Org. Chem 2008;73:644. [PubMed: 18081347] b Lasa M, Jiménez AI, Zurbano MM, Cativiela C. Tetrahedron Lett 2005;46:8377. c Alemán C, Jiménez AI, Cativiela C, Pérez JJ, Casanovas J. J. Phys. Chem. B 2002;106:11849. d Gomez-Catalan J, Jiménez AI, Cativiela C, Perez JJ. J. Pept. Res 2001;57:435. [PubMed: 11437947] e Jiménez AI, Cativiela C, Gómez-Catalán J, Pérez JJ, Aubry A, París M, Marraud M. J. Am. Chem. Soc 2000;122:5811. f Jiménez AI, Cativiela C, Aubry A, Marraud M. J. Am. Chem. Soc 1998;120:9452.
5. a Zanuy D, Jiménez AI, Cativiela C, Nussinov R, Alemán C. J. Phys. Chem. B 2007;111:3236. [PubMed: 17388467] b Crisma M, Toniolo C, Royo S, Jiménez AI, Cativiela C. Org. Lett 2006;8:6091. [PubMed: 17165937] c Crisma M, De Borggraeve WM, Peggion C, Formaggio F, Royo S, Jiménez AI, Cativiela C, Toniolo C. Chem. Eur. J 2006;12:251. d Jiménez AI, Ballano G, Cativiela C. Angew. Chem. Int. Ed 2005;44:396. e Royo S, De Borggraeve WM, Peggion C, Formaggio F, Crisma M, Jiménez AI, Cativiela C, Toniolo C. J. Am. Chem. Soc 2005;127:2036. [PubMed: 15713068]
6. Rodríguez-Ropero F, Zanuy D, Casanovas J, Nussinov R, Alemán C. J. Chem. Inf. Mod 2008;48:333.
7. Alemán C, Zanuy D, Casanovas J, Cativiela C, Nussinov R. J. Phys. Chem. B 2006;110:21264. [PubMed: 17048955]
8. Frisch, MJ.; Trucks, GW.; Schlegel, HB.; Scuseria, GE.; Robb, MA.; Cheeseman, JR.; Montgomery, JA.; Vreven, T., Jr.; Kudin, KN.; Burant, JC.; Millam, JM.; Iyengar, SS.; Tomasi, J.; Barone, V.; Mennucci, B.; Cossi, M.; Scalmani, G.; Rega, N.; Petersson, GA.; Nakatsuji, H.; Hada, M.; Ehara, M.; Toyota, K.; Fukuda, R.; Hasegawa, J.; Ishida, M.; Nakajima, T.; Honda, Y.; Kitao, O.; Nakai, H.; Klene, M.; Li, X.; Knox, JE.; Hratchian, HP.; Cross, JB.; Adamo, C.; Jaramillo, J.; Gomperts, R.; Stratmann, RE.; Yazyev, O.; Austin, AJ.; Cammi, R.; Pomelli, C.; Ochterski, JW.; Ayala, PY.; Morokuma, K.; Voth, GA.; Salvador, P.; Dannenberg, JJ.; Zakrzewski, VG.; Dapprich, S.; Daniels, AD.; C. Strain, M.; Farkas, O.; Malick, DK.; Rabuck, AD.; Raghavachari, K.; Foresman, JB.; Ortiz, JV.; Cui, Q.; Baboul, AG.; Clifford, S.; Cioslowski, J.; Stefanov, BB.; Liu, G.; Liashenko, A.; Piskorz, P.; Komaromi, I.; Martin, RL.; Fox, DJ.; Keith, T.; Al-Laham, MA.; Peng, CY.; Nanayakkara, A.; Challacombe, M.; Gill, PMW.; Johnson, B.; Chen, W.; Wong, MW.; Gonzalez, C.; Pople, JA. Gaussian 03, Revision B.02. Gaussian, Inc.; Pittsburgh PA: 2003.
9. Becke AD. J. Chem. Phys 1993;98:1372.
10. Lee C, Yang W, Parr RG. Phys. Rev. B 1993;37:785.
11. Frich MJ, Pople JA, Krishnam R, Binkley JS. J. Chem. Phys 1984;80:3264.
12. Møller C, Plesset MS. Phys. Rev 1934;46:618.
13. McLean AD, Chandler GS. J. Chem. Phys 1980;72:5639.

14. a Miertus S, Scrocco E, Tomasi J. Chem. Phys 1981;55:117. b Miertus S, Tomasi J. Chem. Phys 1982;65:239. c Tomasi J, Persico M. Chem. Phys 1994;94:2027. d Tomasi J, Mennucci B, Cammi R. *Chem. Rev*. 2005;105:2999. [PubMed: 16092826]

15. a Hawkins GD, Cramer CJ, Truhlar DG. J. Phys. Chem. B 1998;102:3257. b Jang YH, Goddard WA III, Noyes KT, Sowers LC, Hwang S, Chung DS. J. Phys. Chem. B 2003;107:344. c Iribarren JI, Casanovas J, Zanuy D, Alemán C. Chem. Phys 2004;302:77.

16. Perczel A, Angyan JG, Kajtar M, Viviani W, Rivail J-L, Marcoccia J-F, Csizmadia IG. J. Am. Chem. Soc 1991;113:6256.

17. a Kopple KD, Marr DH. J. Am. Chem. Soc 1967;89:6193. [PubMed: 6055982] b Robinson DR, Jencks WP. J. Am. Chem. Soc 1965;87:2470. [PubMed: 14327155]

18. a Gil AM, Buñuel E, Jiménez AI, Cativiela C. Tetrahedron Lett 2003;44:5999. b Halab L, Lubell WD. J. Am. Chem. Soc 2002;124:2474. [PubMed: 11890796] c Tóth G, Murphy RF, Lovas S. J. Am. Chem. Soc 2001;123:11782. [PubMed: 11716735] d Tóth G, Watts CR, Murphy RF, Lovas S. Proteins: Struct. Funct. Genet 2001;43:373. [PubMed: 11340654] e Steiner T, Koellner G. J. Mol. Biol 2001;305:535. [PubMed: 11152611] f Steiner T, Schreurs AMM, Kanters JA, Kroon J. Acta Cryst., Sect. D 1998;54:25. [PubMed: 9761814] g Worth GA, Wade RC. J. Phys. Chem 1995;99:17473. h Mitchell JBO, Nandi CL, McDonald IK, Thornton JM. J. Mol. Biol 1994;239:315. [PubMed: 8196060] i Flocco MM, Mowbray SL. J. Mol. Biol 1994;235:709. [PubMed: 8289290] j Mitchell JBO, Nandi CL, Ali S, McDonald IK, Thornton JM. Nature 1993;366:413. k Singh J, Thornton JM. J. Mol. Biol 1990;211:595. [PubMed: 2308168]

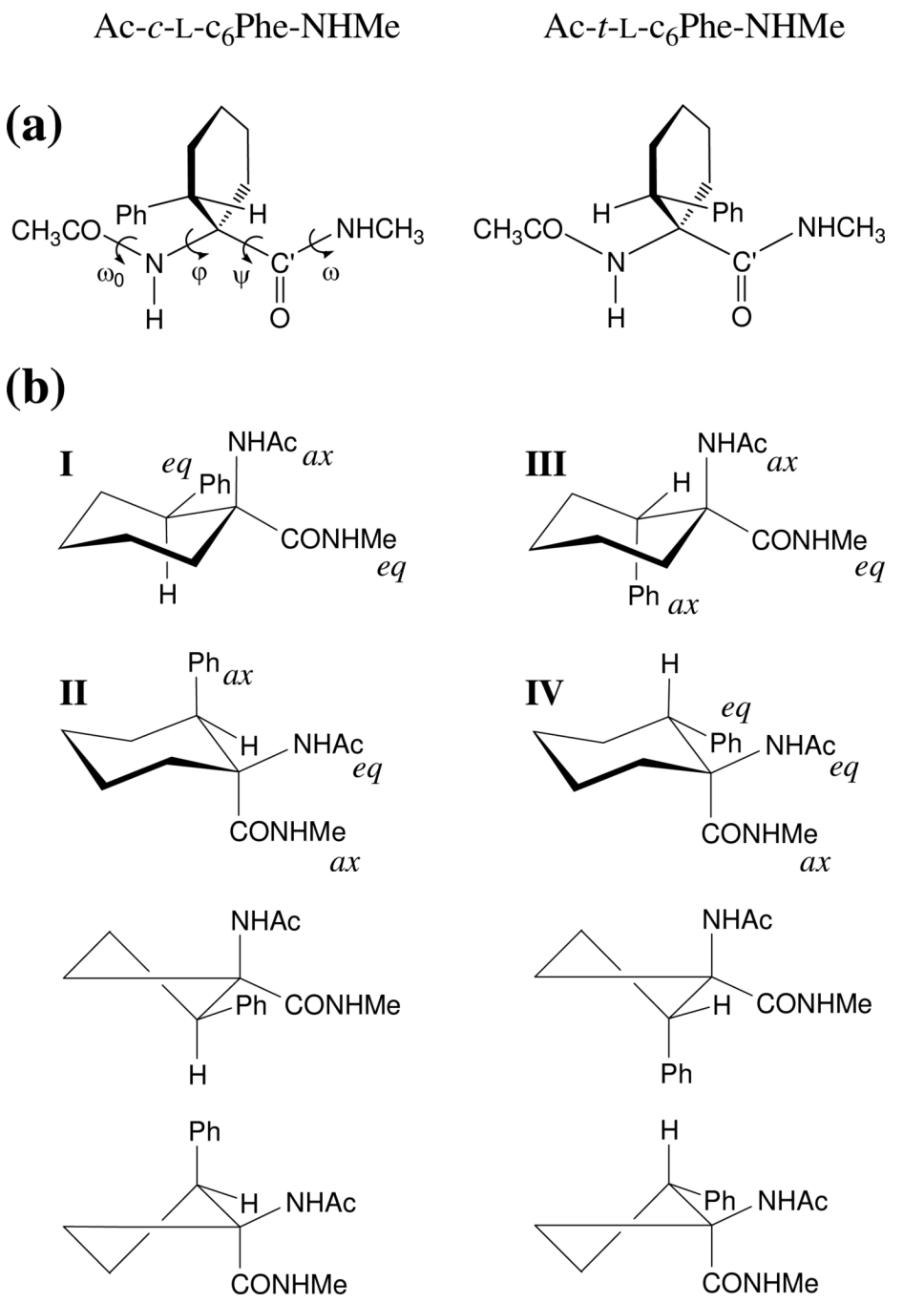

Figure 1.

(a) Structure of the compounds investigated, Ac-*c*-L-c$_6$Phe-NHMe and Ac-*t*-L-c$_6$Phe-NHMe, that incorporate, respectively, the *cis* and *trans* cyclohexane analogues of L-phenylalanine. The backbone dihedral angles are indicated for the *cis* derivative. (b) Chair and half-chair conformations considered as starting geometries for the cyclohexane ring in the compounds under study. The substituents located in axial (*ax*) or equatorial (*eq*) positions are indicated for the chair conformations.

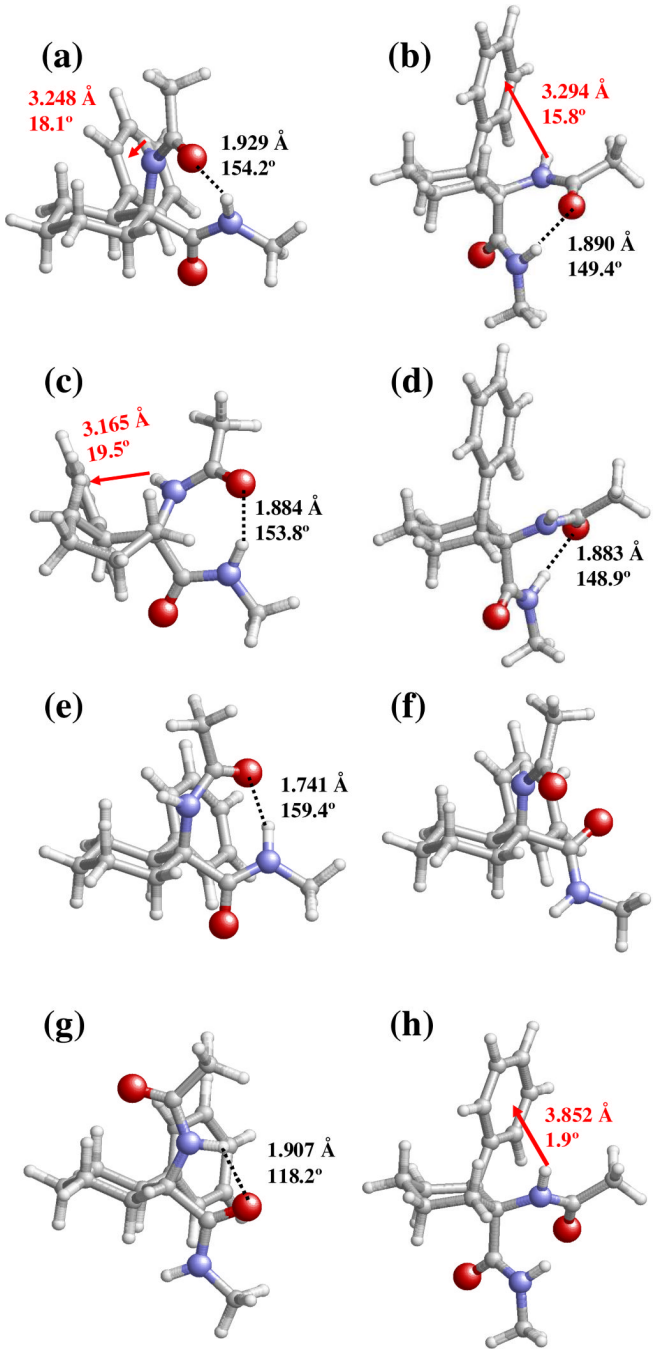

Figure 2.

Selected minimum energy conformations characterized for Ac-*c*-L-c_6Phe-NHMe at the B3LYP/6-31+G(d,p) level: (a) **1**; (b) **2**; (c) **3**; (d) **4**; (e) **5**; (f) **6**; (g) **7**; and (h) **8**. Conformational parameters are provided in Table 1. Intramolecular N–H···O hydrogen bonds and N–H···π interactions are indicated by black dashed lines and red arrows, respectively. The geometrical parameters correspond to the d(H···O) and <N–H···O (in Å and degrees, respectively) for hydrogen bonds and to $d_{H\cdots Ph}$ and θ (in Å and degrees, respectively; see text for definition) for N–H···π interactions.

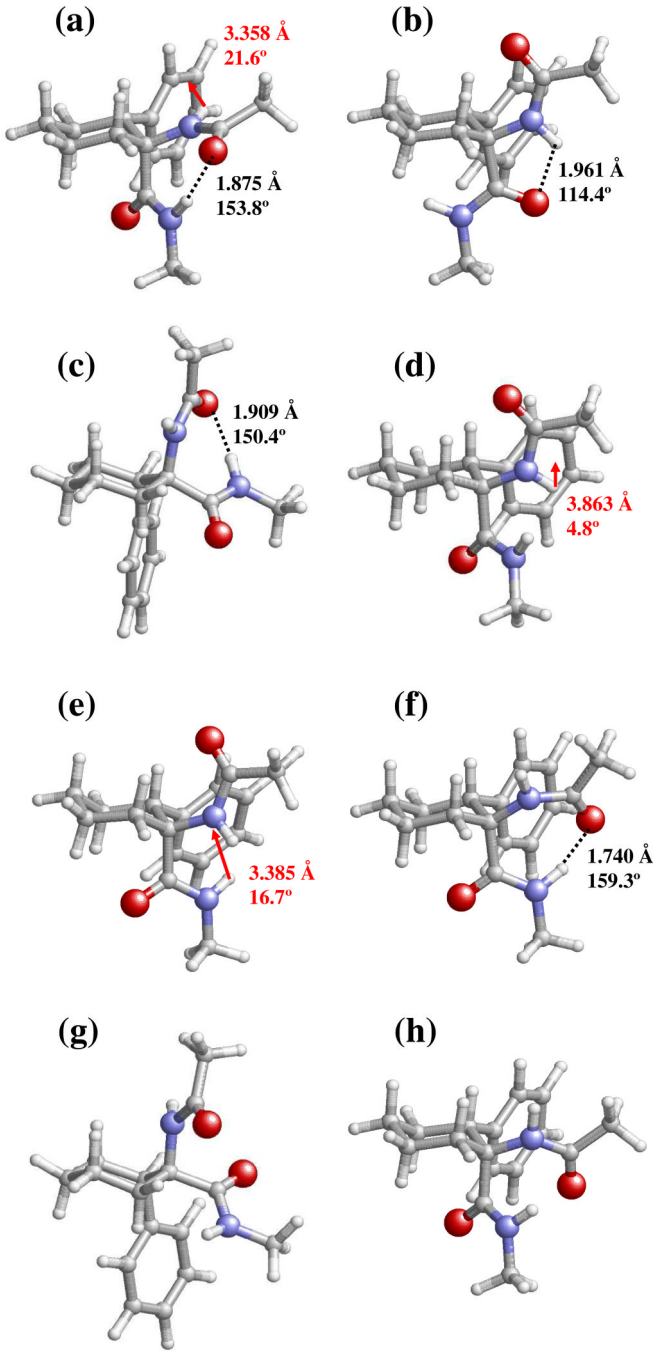

Figure 3.

Selected minimum energy conformations characterized for Ac-*t*-$_L$-c_6Phe-NHMe at the B3LYP/6-31+G(d,p) level: (a) **1**; (b) **2**; (c) **3**; (d) **4**; (e) **5**; (f) **6**; (g) **7**; and (h) **8**. Conformational parameters are provided in Table 2. Intramolecular N–H···O hydrogen bonds and N–H···π interactions are indicated by black dashed lines and red arrows, respectively. The geometrical parameters correspond to the d(H···O) and <N–H···O (in Å and degrees, respectively) for hydrogen bonds and to $d_{H\cdots Ph}$ and θ (in Å and degrees, respectively; see text for definition) for N–H···π interactions.

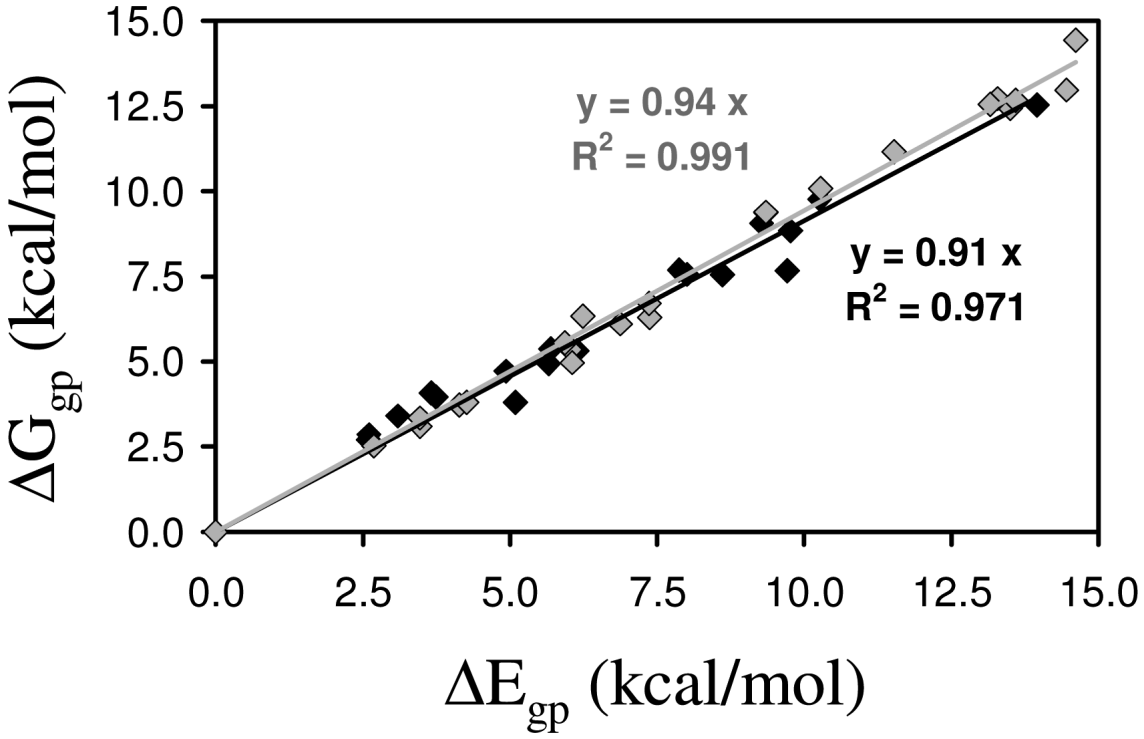

Figure 4.

Graphical representation of ΔE_{gp} *vs*. ΔG_{gp} calculated at the B3LYP/6-31+G(d,p) level for Ac-*c*-L-c$_6$Phe-NHMe (black diamonds) and Ac-*t*-L-c$_6$Phe-NHMe (grey diamonds). The regressions ($y = c \cdot x$) and correlation coefficients (R^2) are displayed for each compound.

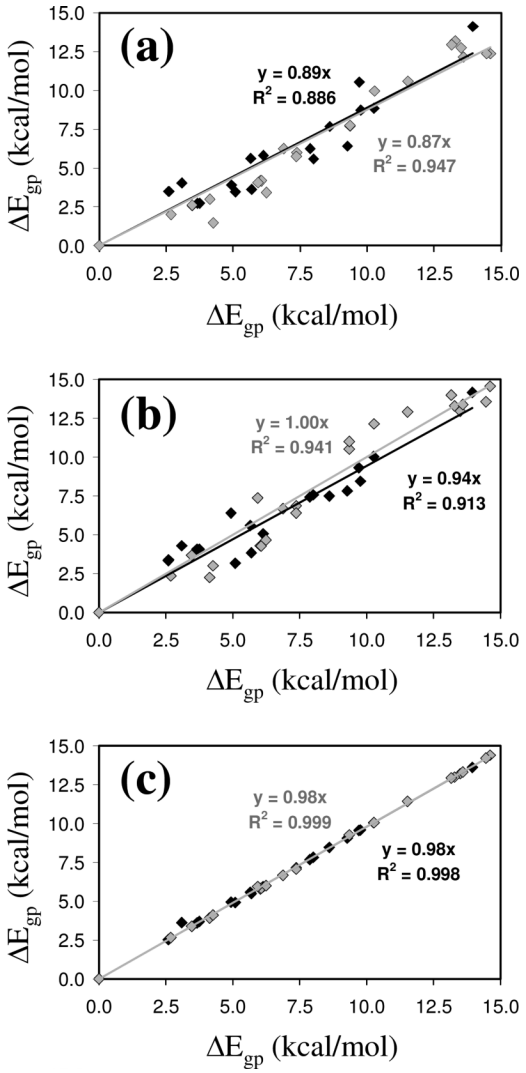

Figure 5.

Graphical representation of ΔE_{gp} calculated at the B3LYP/6-31+G(d,p) level *vs*. ΔE_{gp} predicted at the (a) MP2/6-31+G(d,p), (b) HF/6-31+G(d,p) and (c) B3LYP/6-311++G(d,p) levels for Ac-*c*-L-c$_6$Phe-NHMe (black diamonds) and Ac-*t*-L-c$_6$Phe-NHMe (grey diamonds). The regressions ($y= c \cdot x$) and correlation coefficients (R^2) are displayed for each compound.

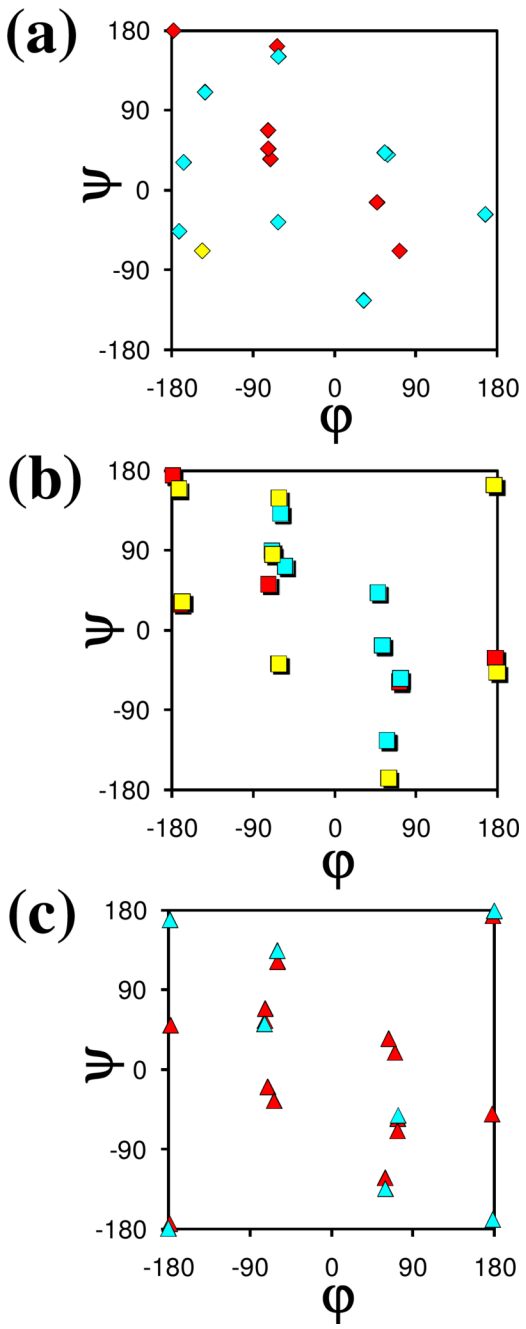

Figure 6.

Comparison between the minimum energy conformations predicted for (a) Ac-*c*-L-c_6Phe-NHMe, (b), Ac-*t*-L-c_6Phe-NHMe and (c) Ac-Ac_6c-NHMe at the B3LYP/6-31+G(d,p) level. Color code: red, $\Delta G_{gp} < 5$ kcal/mol; blue, 5 kcal/mol $\leq \Delta G_{gp} < 10$ kcal/mol; yellow, $\Delta G_{gp} \geq 10$ kcal/mol. For the Ac_6c derivative, both the (φ,ψ) and (–φ,–ψ) positions are indicated for each minimum.

Table 1

Backbone dihedral angles,[a,b] relative energy[c] in the gas phase (ΔE_{gp}), and relative free energy[c] in the gas phase (ΔG_{gp}) for the minimum energy conformations of Ac-*c*-$_L$-c_6Phe-NHMe characterized at the B3LYP/6-31+G(d,p) level. The arrangement adopted by the peptide backbone and the cyclohexane ring[d] is indicated.

#	ω_0	ϕ	ψ	ω	backbone	cyclohexane	ΔE_{gp}	ΔG_{gp}
1	−175.3	−71.0	35.2	172.9	γ_L	chair I	0.0[e]	0.0[f]
2	−173.6	−73.6	67.4	−176.0	γ_L	chair II	2.6	2.7
3	−174.6	−73.5	46.7	176.1	γ_L	twist	3.1	3.4
4	174.5	71.9	−68.5	175.0	γ_D	chair II	3.7	4.1
5	171.5	46.9	−13.7	177.4	γ_D	chair I	4.9	4.7
6	161.1	−63.7	162.0	−177.7	ε_L	chair I	5.1	3.8
7	177.4	−178.2	179.8	−178.3	β_L	chair I	5.6	4.9
8	166.2	59.3	40.2	−175.5	α_D	chair II	5.7	5.4
9	−168.5	−61.8	−35.9	175.6	α_L	chair II	6.1	5.3
10	166.8	167.4	−27.1	−171.9	δ_D	chair I	7.9	7.7
11	−165.4	32.9	−124.0	175.5	ε_D	chair I	8.0	7.5
12	−170.9	−166.4	31.5	171.5	δ_L	twist	8.6	7.5
13	169.9	56.1	42.4	−175.0	α_D	twist	9.3	9.0
14	−174.4	−142.7	110.5	−174.1	δ_L	chair II	9.7	7.7
15	165.3	−61.5	150.8	−177.3	ε_L	twist	9.8	8.8
16	169.5	−171.3	−46.1	−174.1	δ_D	twist	10.3	9.7
17	178.6	−146.0	−68.6	178.3	δ_D	twist	13.9	12.5

[a] In degrees.

[b] See Figure 1a for definition.

[c] In kcal/mol.

[d] See Figure 1b.

[e] E=−883.014845 a.u.

[f] G=−882.701540 a.u.

Table 2

Backbone dihedral angles,[a,b] relative energy[c] in the gas phase (ΔE_{gp}) and relative free energy[c] in the gas phase (ΔG_{gp}) for the minimum energy conformations of Ac-*t*-L-c$_6$Phe-NHMe characterized at the B3LYP/6-31+G(d,p) level. The arrangement adopted by the peptide backbone and the cyclohexane ring[d] is indicated.

#	ω_0	ϕ	ψ	ω	backbone	cyclohexane	ΔE_{gp}	ΔG_{gp}
1	−175.2	−73.5	52.2	178.4	γ_L	chair IV	0.0[e]	0.0[f]
2	179.7	−179.2	175.2	−178.6	β_L	chair IV	2.7	2.5
3	177.6	71.4	−58.2	−178.7	γ_D	chair III	3.5	3.1
4	−169.7	−170.6	29.9	171.7	δ_L	chair IV	4.1	3.7
5	169.5	177.2	−30.9	−173.2	δ_D	chair IV	4.3	3.8
6	168.1	53.0	−16.9	−177.6	γ_D	chair IV	5.9	5.5
7	167.1	−59.6	131.7	−177.7	ε_L	chair III	6.0	5.3
8	164.6	48.1	42.5	−174.4	α_D	chair IV	6.2	6.3
9	175.7	−69.2	89.5	−172.5	γ_L	chair III	6.9	6.1
10	−167.3	58.0	−123.9	175.8	ε_D	chair III	7.4	6.3
11	−170.0	−61.6	−37.5	176.7	α_L	chair III	7.4	6.7
12	−176.2	−54.3	72.4	177.6	γ_L	twist	9.3	9.4
13	177.3	72.8	−54.2	−176.0	γ_D	twist	9.3	9.4
14	−176.2	176.2	164.0	175.0	β_L	chair III	10.3	10.1
15	179.9	−172.1	159.7	174.3	β_L	twist	11.5	11.2
16	176.8	−68.8	85.7	−172.3	γ_L	twist	13.2	12.5
17	−172.4	179.4	−47.5	−172.8	δ_D	twist	13.3	12.7
18	−171.0	−168.7	32.4	172.2	δ_L	twist	13.5	12.4
19	−169.1	−61.7	−38.0	178.3	α_L	twist	13.6	12.7
20	164.5	−61.8	149.3	177.8	ε_L	twist	14.4	13.0
21	−163.0	59.5	−166.7	−177.5	ε_D	twist	14.6	14.4

[a] In degrees.

[b] See Figure 1a for definition.

[c] In kcal/mol.

[d] See Figure 1b.

[e] E=−883.014189 a.u.

[f] G=−882.701217 a.u.

Table 3

Relative energy in the gas phase[a] (ΔE_{gp}) calculated at different theoretical levels[b] for the minimum energy conformations of Ac-*c*-L-c$_6$Phe-NHMe.

#	6-31+G(d,p)			6-311++G(d,p)
	B3LYP	**MP2**	**HF**	**B3LYP**
1	0.0[c]	0.0[d]	0.0[e]	0.0[f]
2	2.6	3.5	3.3	2.5
3	3.1	4.0	4.3	3.6
4	3.7	2.7	4.1	3.6
5	4.9	3.9	6.4	4.9
6	5.1	3.5	3.2	4.9
7	5.6	5.6	5.6	5.6
8	5.7	3.6	3.8	5.5
9	6.1	5.8	5.1	5.9
10	7.9	6.2	7.4	7.7
11	8.0	7.8	5.6	7.6
12	8.6	7.7	7.5	8.5
13	9.3	6.4	7.8	9.1
14	9.7	10.5	9.3	9.6
15	9.8	8.7	8.4	9.6
16	10.3	8.9	10.0	10.0
17	13.9	14.1	14.1	13.6

[a] In kcal/mol.

[b] Energies at the MP2/6-31+G(d,p), HF/6-31+G(d,p) and B3LYP/6-311++G(d,p) levels were derived from single point calculations on B3LYP/6-31+G(d,p) geometries.

[c] E=−883.014845 a.u.

[d] E=−880.353232 a.u.

[e] E=−877.425595 a.u.

[f] E=−883.196342 a.u.

Table 4

Relative energy in the gas phase[a] (ΔE_{gp}) calculated at different theoretical levels[b] for the minimum energy conformations of Ac-*t*-$_L$-c_6Phe-NHMe.

#	6-31+G(d,p)			6-311++G(d,p)
	B3LYP	**MP2**	**HF**	**B3LYP**
1	0.0[c]	0.0[d]	0.0[e]	0.0[f]
2	2.7	2.0	2.3	2.6
3	3.5	2.6	3.7	3.4
4	4.1	3.0	2.2	3.9
5	4.3	1.5	3.0	4.2
6	5.9	4.1	7.3	5.9
7	6.0	4.2	4.3	5.8
8	6.2	6.0	3.4	4.7
9	6.9	6.7	6.2	6.7
10	7.4	7.1	6.0	6.9
11	7.4	5.7	6.4	7.1
12	9.3	7.7	10.5	9.2
13	9.3	7.7	11.0	9.3
14	10.3	9.9	12.1	10.0
15	11.5	10.6	12.9	11.4
16	13.2	12.9	14.0	12.9
17	13.3	13.2	13.3	13.0
18	13.5	12.7	12.9	13.2
19	13.6	12.1	13.4	13.3
20	14.4	12.4	13.6	14.2
21	14.6	12.3	14.6	14.4

[a] In kcal/mol.

[b] Energies at the MP2/6-31+G(d,p), HF/6-31+G(d,p) and B3LYP/6-311++G(d,p) levels were derived from single point calculations on B3LYP/6-31+G(d,p) geometries.

[c] E=−883.014189 a.u.

[d] E=−880.351683 a.u.

[e] E=−877.424807 a.u.

[f] E=−883.195613 a.u.

Table 5

Relative conformational free energies[a] at 298 K for the minimum energy conformations of Ac-*c*-L-c$_6$Phe-NHMe in the gas phase ($\Delta G_{gp,*}$),[b] chloroform solution (ΔG_{Chl}) and aqueous solution (ΔG_{water}). The solvation free energies[a] in chloroform and aqueous solutions [ΔG_{solv}(Chl) and ΔG_{solv}(water), respectively] are also given.

#	$\Delta G_{gp,*}$	ΔG_{solv}(Chl)	ΔG_{Chl}	ΔG_{solv}(water)	ΔG_{water}
1	0.0[c]	2.8	0.6	4.7	5.5
2	3.6	2.5	3.9	4.5	8.9
3	4.3	3.1	5.2	5.5	10.6
4	3.1	1.0	2.0	1.2	5.2
5	3.7	2.0	3.5	1.5	6.0
6	2.2	0.0	0.0	−2.2	0.8
7	4.9	0.3	3.0	−1.5	4.2
8	3.3	−1.0	0.1	−4.1	0.0
9	5.0	0.9	3.7	−0.5	5.3
10	6.1	1.4	5.3	−0.4	6.5
11	5.1	0.4	3.3	−0.5	5.4
12	6.6	1.3	5.7	0.2	7.6
13	6.2	−1.4	2.6	−5.0	2.0
14	8.5	0.5	6.8	−0.6	8.7
15	7.8	1.0	6.6	−0.4	8.2
16	8.4	−1.4	4.8	1.1	10.3
17	12.7	−0.3	10.2	−4.6	8.9

[a] In kcal/mol.

[b] $\Delta G_{gp,*}$ corresponds to the best estimation of ΔG_{gp}, which was obtained by combining the ΔE_{gp} value calculated at the MP2/6-31+G(d,p) level with the thermodynamic corrections obtained at the B3LYP/6-31+G(d,p) level.

[c] G= −880.039927 a.u.

Table 6

Relative conformational free energies[a] at 298 K for the minimum energy conformations of Ac-*t*-L-c$_6$Phe-NHMe in the gas phase ($\Delta G_{gp,*}$),[b] chloroform solution (ΔG_{Chl}) and aqueous solution (ΔG_{water}). The solvation free energies[a] in chloroform and aqueous solutions [ΔG_{solv}(Chl) and ΔG_{solv}(water), respectively] are also given.

#	$\Delta G_{gp,*}$	ΔG_{solv}(Chl)	ΔG_{Chl}	ΔG_{solv}(water)	ΔG_{water}
1	0.0[c]	3.3	1.0	5.3	6.2
2	1.8	1.3	0.8	1.7	4.4
3	2.2	1.0	0.9	0.5	3.6
4	2.6	1.7	1.9	−0.7	2.7
5	1.0	1.5	0.2	0.4	2.3
6	3.7	1.4	2.8	0.0	4.6
7	3.5	−0.3	0.9	−2.1	2.3
8	3.5	−1.2	0.0	−4.4	0.0
9	5.5	0.6	3.8	−0.8	5.6
10	4.9	0.9	3.5	0.3	6.1
11	5.1	−1.3	1.5	−5.5	0.5
12	7.7	1.2	6.6	1.1	9.7
13	7.8	0.5	5.9	0.5	9.1
14	9.7	1.3	8.7	2.1	12.7
15	10.2	1.3	9.2	2.5	13.6
16	12.3	0.2	11.5	−0.8	10.2
17	13.1	0.6	11.4	−1.5	12.5
18	11.7	0.2	9.6	−0.9	11.7
19	11.2	−1.8	7.1	−6.7	5.4
20	10.9	−1.1	7.5	−3.4	8.4
21	12.2	−0.5	9.3	0.2	13.2

[a] In kcal/mol.

[b] $\Delta G_{gp,*}$ corresponds to the best estimation of ΔG_{gp}, which was obtained by combining the ΔE_{gp} value calculated at the MP2/6-31+G(d,p) level with the thermodynamic corrections obtained at the B3LYP/6-31+G(d,p) level.

[c] G= −880.038710 a.u.